

Deflagration-to-Detonation Transition for Hydrogen-Enriched Air Mixtures through Pressure Wave Focusing in Pipes

S. Bengoechea, J.A.T. Gray, J. Reiss, J.P. Moeck, C.O. Paschereit, J. Sesterhenn
 Institut für Strömungsmechanik und Technische Akustik ISTA, TU-Berlin, Germany

1 Introduction

The use of detonation presents a more efficient alternative of releasing the chemical energy of fuel-oxidizer mixtures. The cornerstone of pulse-detonation-engines (PDEs) is the ability of producing a reliable deflagration-to-detonation transition (DDT) over a short distance. This is imperative for the application in gas turbines.

This report describes the experimental and numerical study of DDT in a pipe obstructed by a single obstacle (an axisymmetric convergent-divergent nozzle as described in [1]). This nozzle is similar to that used by Frolov et al. [2]. The combustion chamber is filled with a mixture of hydrogen-air, enriched to 40% oxygen ($\frac{4}{9}H_2 + \frac{2}{9}O_2 + \frac{3}{9}N_2$). The effects the proposed configuration has on the onset of detonation for PDEs has been analysed. For this purpose, different scenarios have been confronted, thereby, enhancing the understanding of the processes inside the pipe and bringing closer experiments and simulation by the use of data assimilation techniques [3]. For one of the cases, the necessary parameters for a successful DDT are identified and the results indicate a close to 100% rate of success in the transition. This deterministic and reliable behaviour paves the way for a potential use in PDEs.

2 Methods

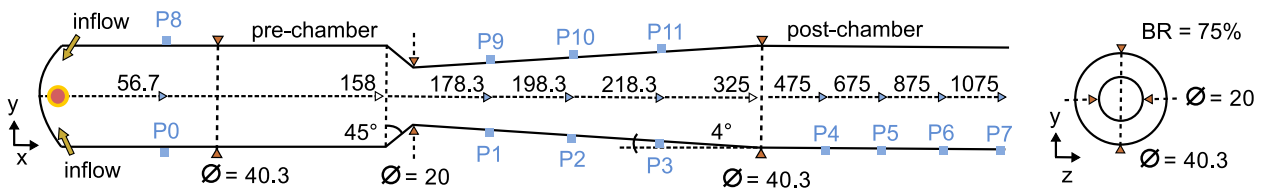


Figure 1: Diagram of the configuration under investigation, all dimensions in mm. Measurement points are marked with P. Ignition spot at the left boundary (red circle). The Blockage-Ratio (BR) is 75%.

2.1 Experimental Setup

Figure 1 depicts a schematic of the configuration under analysis. One single obstacle (a convergent-divergent nozzle) separates the pre-chamber and the post-chamber and the supply of the reactive mixture

occurs through a 0.5 mm circumferential slot at the upstream side (left). The obstacle design allows for the leading shock ahead of the turbulent flame to be focused at the center of the convergent section of the nozzle. Twelve piezo-electric pressure transducers (PCB 112A05) were installed at various positions in order to capture the pressure evolution in the chamber, see Figure 1. The pre-chamber is also equipped with a transparent window in front of the obstacle. The experimental facility has two running modes: 1) the quiescent mode, in which the detonation chamber is evacuated and filled using partial pressures, resulting in a case for which the flow is initially at rest and 2) the filling mode, in which a continuous supply of the mixture produces turbulent initial conditions, reproducing the multi-cycle operating mode in PDEs more closely.

2.2 Numerical Methods

The reactive Navier-Stokes equations for compressible gaseous mixtures including the effects of viscosity, thermal conduction, diffusion and chemical reaction are numerically solved. The shear viscosity is calculated with the Sutherland law in order to implement the viscosity temperature dependence in the gases. The species diffusion is described by Fick's law and the chemical kinetics by a one-step irreversible reaction, based on the Arrhenius model. A constant adiabatic exponent is assumed and the Lewis number is considered to be equal to one. The validation of the physical-chemical equation model was confirmed against the adiabatic laminar flame and the CJ detonation. These are not included in the report, due to space limitations.

The geometry depicted in Figure 1 is mapped onto a two-dimensional domain with approximately 8 million points and solved with the in-house code, fully parallelized by means of MPI at 512 CPUs [4]. An explicit central scheme of 4-th order is applied to all spacial derivatives and the solution has been time integrated with the 4-th order explicit Runge-Kutta method. All the boundaries are set to non-slip adiabatic walls, except for the open end on the right, where the outflow is non-reflecting.

As well as in the experimental measurements, two cases are simulated, *Case A* corresponds to a quiescent mode, resulting in an initially laminar flame. The data assimilation is applied to *Case B*, with the experimental results taken as reference [3]. The high burning rate, characteristic of turbulent flames, is modelled by the increase of mass and heat diffusion maintaining the unit of the Lewis number. The start temperature at the point of ignition is set within an area of 3 mm^2 to 1100 K and 2000 K in *Case A* and *B*, respectively. The other initial quantities are at rest with $T_0 = 298.15 \text{ K}$ and $p_0 = 101330 \text{ Pa}$.

3 Results

Case A: Figure 2 shows the temporal pressure records for the experiment and the simulation, averaged over the two opposite sensors. A similar growth in the initial phase until 2.5 ms is observed for the sensors P0 & P8. The pressure rise in the pre-chamber is related to the flame expansion due the piston-effect and the pressure wave reflections. The major deviation is the run-up distance to DDT. In the simulation the transition appears just downstream of the obstacle, seen in Figure 2 at the sensor pair P1 & P9. While the experimental results show a detonation farther downstream at sensor P4.

The numerical results present a highly unsteady scenario with shock-turbulent flame interactions, creating ignition centers (hot-spots) in the unreacted mixture. The existence of an inhomogeneous reactivity gradient at these centers restructures the flame into a detonation by the Zeldovich's gradient mechanism [5]. However, the one-step kinetics model makes strong assumptions by the parameter fitting, which underestimate the induction time τ_c and unnaturally supports the DDT [6]. Such deficiencies explain the mismatch of the

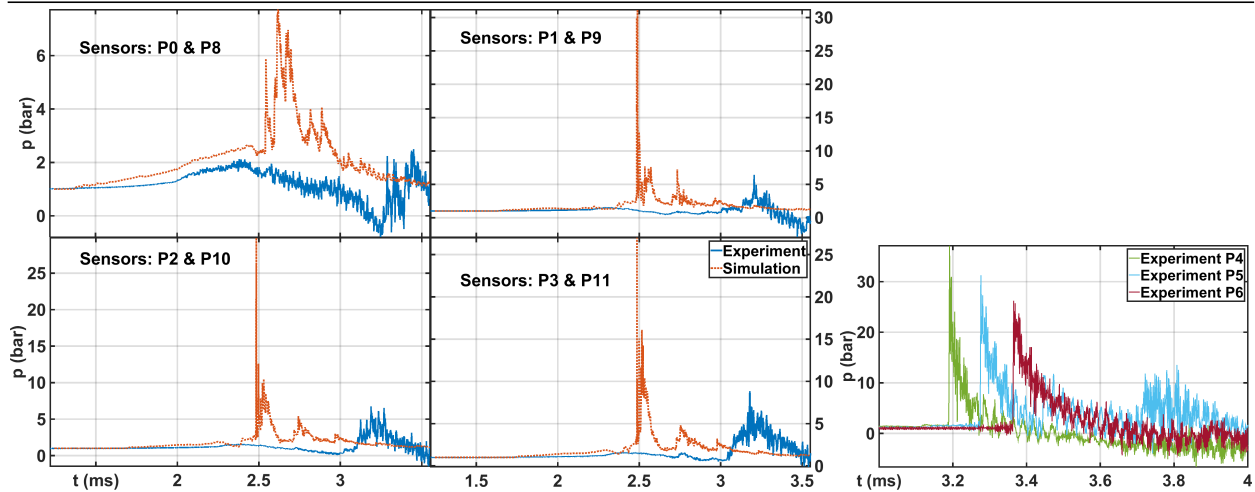


Figure 2: Pressure records averaged over the pairs of measurement points: P0 & P8, P1 & P9, P2 & P10, P3 & P11 and P4, P5, P6.

run-up distance to DDT between the experimental and numerical results of Figure 2. The one-step model reproduces accurately the deflagration and detonation propagation fronts, but fails to capture the transition process between them. Additionally, in the experiment for *Case A* the transition appears further downstream, where the obstacle influence on the DDT is residual.

Case B: Figure 3 plots the pressure averaged over opposed sensors (solid blue line). The signal recorded at sensors P0 & P8 indicates a rapid increase of the pressure in the pre-chamber, which denotes the high turbulent combustion rate, supporting the formation of a strong leading shock wave. These same sensors (P0 & P8) show the retonation wave after the DDT at 1.43 ms and the left boundary reflection at 1.5 ms. In Figure 3, the sensors P1 & P9 depict the detonation wave and a very short precursor pressure step in front of it.

The resulting curves for the assimilated simulation are presented in Figure 3 as well (dotted red line). After the flame modelling, the pressure increase in the pre-chamber is achieved at the sensor pair P0 & P8. The simulated records at P1 & P9 capture the leading shock around 1.375 ms but there is no detonation front afterwards.

The lacking energy to trigger DDT at the focusing point in the simulation is a two-dimensional outcome and to compensate it the activation energy of the model is adjusted. To this end, a statistical estimation based on wave velocities, sensor positions, and time delays was used to evaluate the origin of DDT. This preliminary estimation situates the DDT location right before sensors P1 & P9, which is consistent with the pressure record at P1 & P9 of Figure 3. After the second data fitting there is an excellent matching between numerical and experimental results for all sensors, see Figure 3 (dotted yellow line).

Figure 4 shows two numerical schlieren results after DDT. The upper plot depicts the focusing of the leading shock at the throat as the initiator of DDT. Note the detonation front following closely the leading shock at P1 & P9 location in the upper plot. In particular *Case B* is described by: 1) a high burning rate to create a strong leading shock wave with a velocity of approximately 800 m/s at the nozzle inlet (numerically obtained) and 2) its focusing due the geometry. Figure 5 depicts a serie of high-speed experimental images

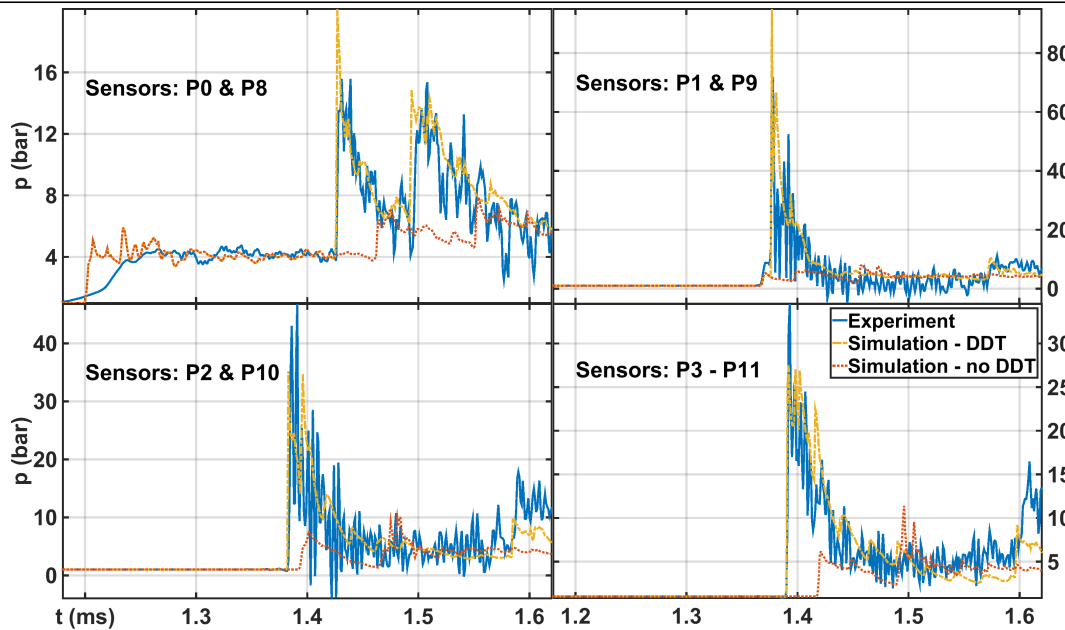


Figure 3: Pressure records averaged over the pairs of points: P0 & P8, P1 & P9, P2 & P10, P3 & P11.

of the flame at the pre-chamber. A source of light appears at the right end where the nozzle is located before the turbulent flame reaches it and leaves the leading pressure front as the only possible trigger mechanism. The numerical and experimental results of Figures 4 and 5 are consistent and complete a solid description of DDT for *Case B*.

The experimental results delivered a 96 % of DDT success, and similar temporal pressure records. The standard deviation of the detonation arrival at sensor P4 is 0.7 % of the mean value, which makes the event close to deterministic.

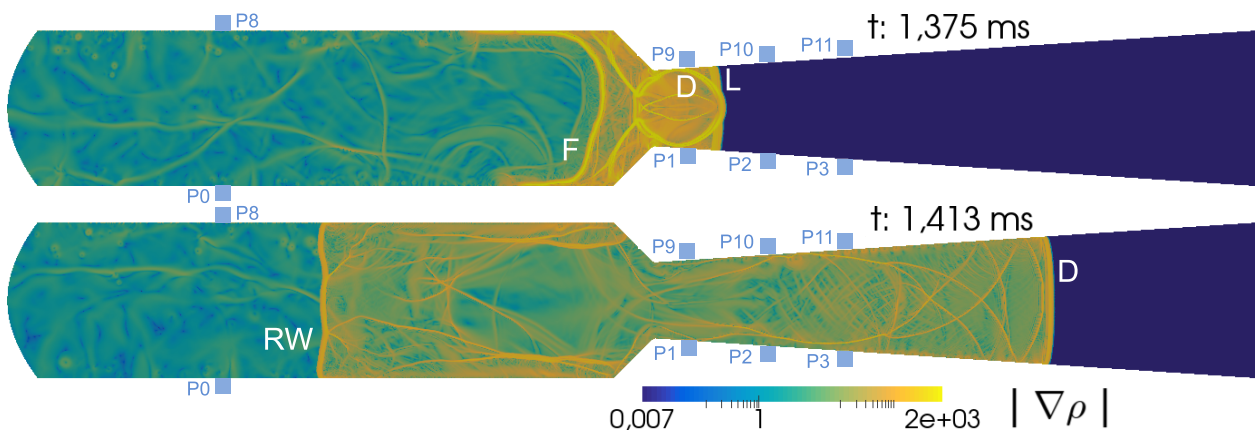


Figure 4: Numerical schlieren of the DDT for the assimilated model. P: sensor points, F: deflagration front, L: leading pressure wave, RW: retonation wave, D: detonation.

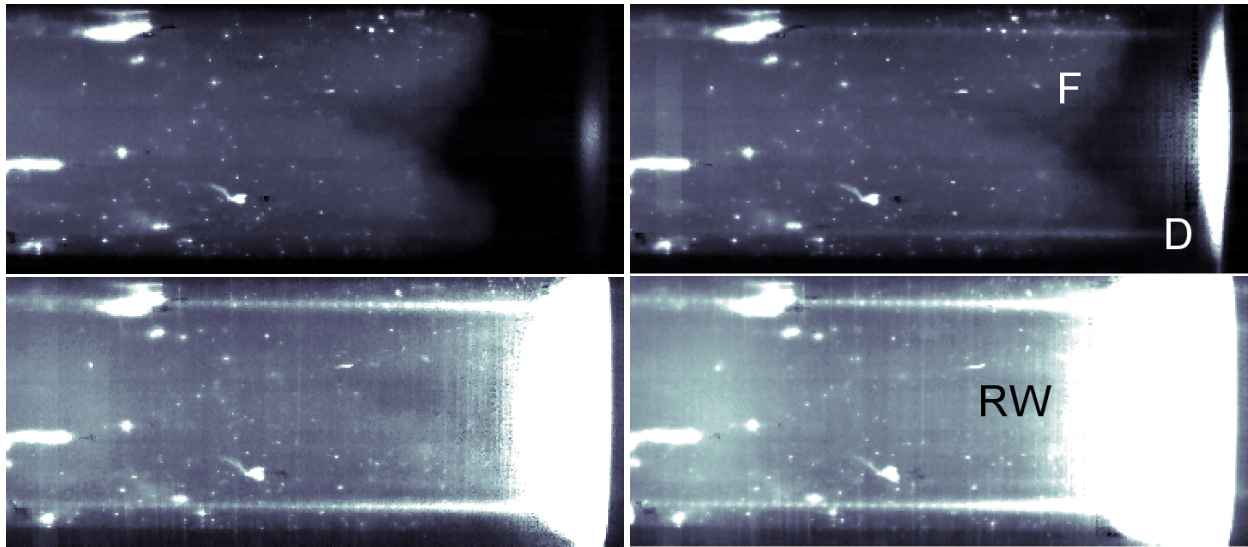


Figure 5: The temporal evolution of the flame up to DDT with $dt = 5$ s. F: deflagration front, D: detonation, RW: retonation wave.

4 Discussion

If the focusing of the leading shock wave at the throat is the trigger mechanism of DDT, there must exist a temporal coherence between τ_c and the time that the high pressure lasts at the focusing point. In order to investigate this, a three-dimensional non-reacting simulation of the interaction of the leading shock wave and the nozzle was executed. The results of Figure 6 depict pressure and temperature over time at the focusing point and show the temporal interval with values over 150 bar and 1450 K to be $4 \cdot 10^{-4}$ ms. The isobaric prediction of the Connaire et al. kinetics model [7], delivers a $\tau_c = 6 \cdot 10^{-4}$ ms for the highest conditions of the focusing point. The temporal scales agree in the order of magnitude and establish the DDT mechanism through the focusing wave as a solid hypothesis.

5 Conclusions

The DDT phenomenon in the present configurations was analysed by combining numerical results and experimental measurements. In *Case A* the divergence between experiment and simulation, the chaotic component in DDT, and the longer run-up distances makes it of minor interest for PDE applications. The results for *Case B* show a reliable and predictable DDT. Therefore, it is of great interest to extend the study to complex chemical kinetics.

Acknowledgements: This work is funded by the Deutsche Forschungsgemeinschaft *DFG* as part of the *SFB-1029* "Substantial efficiency increase in gas turbines through direct use of coupled unsteady combustion and flow dynamics". The computations were executed at the *Leibniz-Rechenzentrum*, ID-Project *pr83lu*.

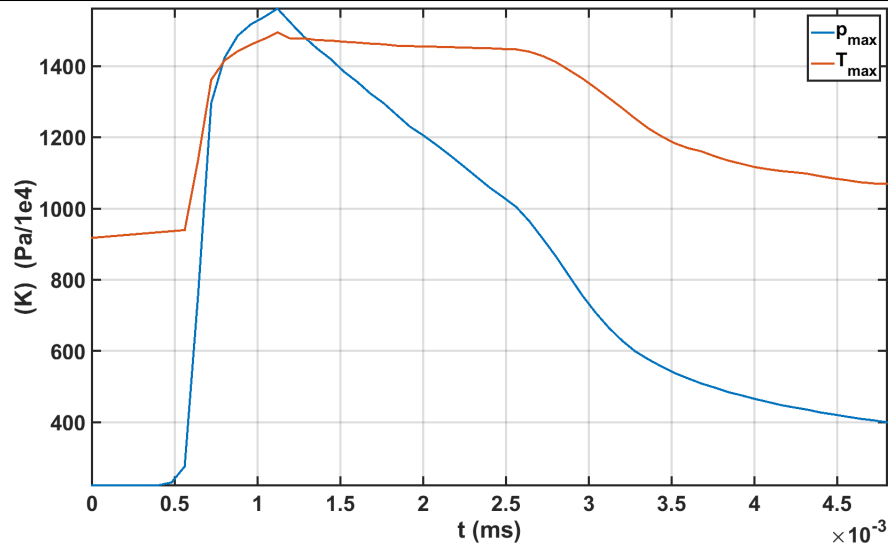


Figure 6: Temperature and pressure profiles over time at the focusing point, extracted from the three-dimensional simulation.

References

- [1] J.A.T. Gray, M. Lemke, J.P. Moeck, J. Reiss, C.O. Paschereit, J. Sesterhenn (2016). A compact shock-focusing geometry for detonation initiation: Experiments and adjoint-based variational data assimilation. Preprint submitted to Combustion and Flame.
- [2] S.M. Frolov, V.S. Aksenov (2009). Initiation of gas detonation in a tube with a shaped obstacle. Doklady Physical Chemistry, Vol. 427, Part 1:129-132.
- [3] M. Lemke (2015). Adjoint based data assimilation in compressible flows with application to pressure determination from PIV data. Institut für Strömungsmechanik und Technische Akustik ISTA. Technische Universität Berlin.
- [4] J. Reiss, J. Sesterhenn (2014). A conservative, skew-symmetric finite difference scheme for the compressible NavierStokes equation. Computers & Fluids 101:208-219.
- [5] E.S. Oran, V.N. Gamezo (2007). Origins of the deflagration-to-detonation transition in gas-phase combustion. Combustion and Flame, 148:4-47.
- [6] M.A. Liberman, A.D. Kiverin, M.F. Ivanov (2012). Regimes of chemical reaction waves initiated by nonuniform initial conditions for detailed chemical reaction models. Physical Review E 85, 056312.
- [7] M.O. Connaire, H.J. Curran, J.M. Simmie, W.J. Pitz, C.K. Westbrook (2004). A Comprehensive Modeling Study of Hydrogen Oxidation. International Journal of Chemical Kinetics, 36:603-622.